Sensors and Actuators A 163 (2010) 315–322

Contents lists available at ScienceDirect

Sensors and Actuators A: Physical

journal homepage: www.elsevier.com/locate/sna

Design and fabrication of a PET/PTFE-based piezoelectric squeeze mode drop-on-demand inkjet printhead with interchangeable nozzle

E.Q. Li[a,*], Q. Xu[a], J. Sun[a], J.Y.H. Fuh[a], Y.S. Wong[a], S.T. Thoroddsen[a,b]

[a] Department of Mechanical Engineering, National University of Singapore, 9 Engineering Drive 1, Singapore 117575, Singapore
[b] Mechanical Engineering, King Abdullah University of Science and Technology, Thuwal, Saudi Arabia

ARTICLE INFO

Article history:
Received 28 January 2010
Received in revised form 4 June 2010
Accepted 22 July 2010
Available online 30 July 2010

Keywords:
Drop-on-demand
Inkjet printing
Interchangeable nozzle
Piezoelectric droplet generator

ABSTRACT

A PET/PTFE-based piezoelectric squeeze mode drop-on-demand inkjet printhead with interchangeable nozzles is designed and fabricated. The printhead chamber is comprised of PET (polyethylene terephthalate) tubing or PTFE (polytetrafluoroethylene, or Teflon) tubing, which of a much softer material, than the conventionally used glass tubing. Applying the same electrical voltage, PET/PTFE-based printhead will generate a larger volume change in the material to be dispensed. The novel printhead fabricated herein has successfully dispensed liquids with viscosities up to 100 cps, as compared to 20 cps for the commercial printheads. Furthermore, PTFE-based printhead provides excellent anti-corrosive property when strongly corrosive inks are involved. The interchangeable nozzle design enables the same printhead to be fitted with nozzles of different orifice size, thus a clogged nozzle can be easily removed for cleaning or replacement. The characteristics of this novel printhead are also studied by dispensing glycerin–water solutions.

1. Introduction

Due to its advantages in automation, low cost, non-contact and ease of material handling, the application of drop-on-demand (DOD) inkjet printing technology has been expanded from conventional graphic printing to new areas, such as fabrication of integrated circuits (ICs) [1,2], LED [3], rapid prototyping (RP) [4], MEMS, cell printing [5–7] and drug delivery [8]. Accordingly, the dispensed liquids have been expanded from the conventional pigmented ink (or standard dye-based ink) to polymers [9–12], gels, cell ink or other materials which often have higher viscosities or even contain large particles or cells.

Consequently, the traditional inkjet printer designed for graphic printing is unable to fulfill the new challenges, one of which is to dispense fluids of very high viscosities. For most of the commercial inkjet printheads supplied by companies like Microdrop, Microfab, Dimatix and XAAR, only liquids with viscosities lower than 20 cps [12] can be consistently dispensed. Fluids with even higher viscosities have to be diluted before printing or warmed up during the printing, which will adversely affect the properties of the liquids.

Another challenge is raised by nozzle clogging. Fluids containing particles, or cells, can easily block the nozzle orifice, resulting in time-consuming nozzle cleaning or even damage of the entire conventional printhead. To solve the problem, the easiest way is to use a nozzle with a bigger orifice, as bigger orifices are less likely to clog. However, this is often not desirable in inkjet printing as bigger nozzles result in bigger droplets and lower printing resolution. In [13], Chen and Basaran reported that by judiciously controlling the piezoelectric parameters governing the flow within the nozzle and thereby the drop formation, droplets with diameters less than 40% of the orifice diameter could be produced. A similar study was carried out by Goghari and Chandra [14]. These studies reveal a possible way to solve this nozzle clogging problem without sacrificing printing resolution. However, their methods only work over a limited range of Ohnesorge numbers.

The poor printability and nozzle clogging may result in unreliable or failed dispensing when using the traditional inkjet printhead design for complex liquids.

In this paper, we will present an in-house-developed PET/PTFE-based piezoelectric squeeze mode inkjet printhead with an interchangeable nozzle design. PET (polyethylene terephthalate) tubing, comprising of a much softer material, is used as the printhead chamber to substitute for the conventionally used glass tubing [15]. Liquids with viscosities of up to 100 cps have been successfully dispensed by this novel printhead. When strongly corrosive inks are involved, Teflon tubing is served as the printhead chamber. The interchangeable nozzle design allows one to easily clean

* Corresponding author. Tel.: +65 97546052; fax: +65 67791459.
E-mail address: g0501019@nus.edu.sg (E.Q. Li).

0924-4247/$ – see front matter © 2010 Elsevier B.V. All rights reserved.
doi:10.1016/j.sna.2010.07.014

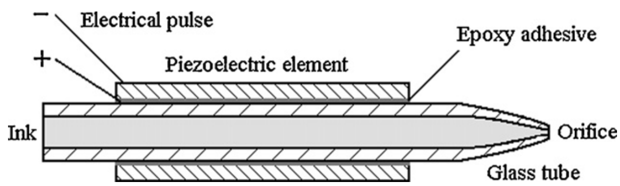

Fig. 1. Schematic showing the construction of a traditional piezoelectric squeeze mode printhead.

or change the clogged or damaged nozzle, avoiding the destruction of the whole printhead assembly.

2. Printhead fabrication

Fig. 1 schematically shows the construction of a traditional piezoelectric squeeze mode printhead. By using epoxy adhesive, a piezoelectric element is tightly attached onto a glass tube which with an orifice at one end. When an electrical pulse is applied, the piezoelectric element will contract inward, squeezing the glass tube as well as the liquid inside. In order to eject a droplet from the orifice, the volume change within the piezoelectric transducer, due to the electrical pulse, must exceeds the volume of liquid to be ejected. Furthermore, the volume change must be sufficient to develop enough pressure inside the liquid to overcome the surface tension at the orifice. The fractional volume change due to the piezoelectric effect is approximately:

$$\frac{\Delta V}{V} = -3d_{31}\frac{U}{t} \qquad (1)$$

where d_{31} is the piezoelectric strain constant, U is the applied voltage and t is the thickness of the piezoelectric tube [16]. The negative sign indicates contraction when the applied pulse has the same polarity as the original polarizing voltage for the piezoelectric element. Eq. (1) shows that the printability of a printhead is mainly depended on the piezoelectric strain constant and the geometry of the piezoelectric transducer. In this study, we focus on how to improve the printability of piezoelectric squeeze printheads without pursuing high piezoelectric strain constant. All the piezoceramic tubes (PZT-5H, from Boston Piezo-Optics Inc.) have the same piezoelectric strain constant d_{31}, approximately -275×10^{-12} m/V, at 25 °C.

The basic idea is to reduce the energy loss during the deformation of the liquid chamber, by replacing the traditionally used glass tube with PET or Teflon tube. Accordingly, the printhead is divided into two parts: a printhead chamber and an interchangeable nozzle attachment fitted tightly to the chamber by screw threading. These will now be described in turn.

2.1. Printhead chamber

The design of the printhead chamber is illustrated in Fig. 2a. The PET heat-shrink tubing has a relative low shrinking temperature ranges from 85 °C to 190 °C. Thus a hair drier is recommended to be the heat source, rather than a burner which could burn up the tubing if overheated. To get a uniform shrunken tubing with a desired diameter, a steel tube with 4.9 mm OD is inserted into the PET tubing during the heating process, as a mould. The PET tube with 6.0 mm OD and 0.1 mm wall thickness (230400CHGS, from Advanced Polymers, Inc.) is evenly heated, shrinking it to a tubing with approximately 5.2 mm OD, so that it can fit exactly inside the piezoceramic tube. This shrunken PET tubing is used as the inner wall for the printhead chamber, which directly contacts with the liquid to be dispensed. By using electrical conductive epoxy (CW2400, from ITW Chemtronics Inc.), the shrunken PET tubing is glued to the inner wall of the piezoceramic tube (PZT-5H, from Boston Piezo-Optics Inc.) with 6.35 mm OD, 0.5 mm wall thickness and 25.4 mm in length.

Teflon tubing serves as the printhead chamber when strongly corrosive inks are involved, due to its perfect anti-corrosive property; however, it is such a non-stick material to be directly bonded to the inner surface of the piezoceramic tube. Fortunately, sodium-based chemical etchant can be used to etch the surfaces of the Teflon material, to make it bondable to another material. In this study, the PrimeEtch® Plus solution, provided by Plastomer Technologies, an EnPro Industries company, is used as the etchant. Teflon tubing (from Zeus, Inc.) with 5.22 mm OD and 0.25 mm wall thickness is dipped into the etchant for 5 min. The etching takes place to a depth of a few hundred angstroms and modifies only the surface composition of the Teflon tubing, leaving other properties of the tubing unaffected, even the dimensions. The etched Teflon tube is then rinsed in alcohol for 2 min, dried, and glued to the inner wall of the piezoceramic tube by using electrical conductive epoxy

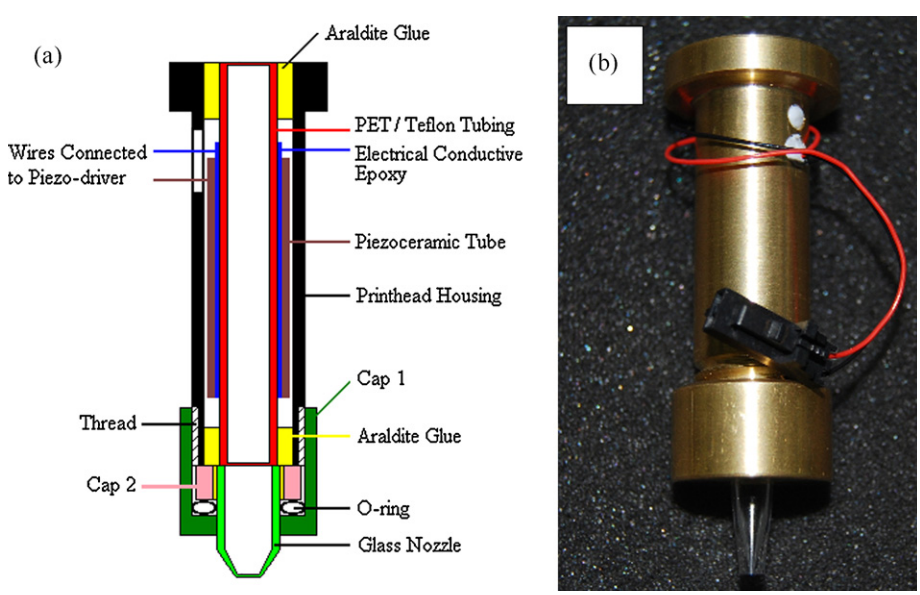

Fig. 2. The novel printhead: (a) schematic showing of the design (out of proportion). (b) A self-fabricated printhead following the novel design.

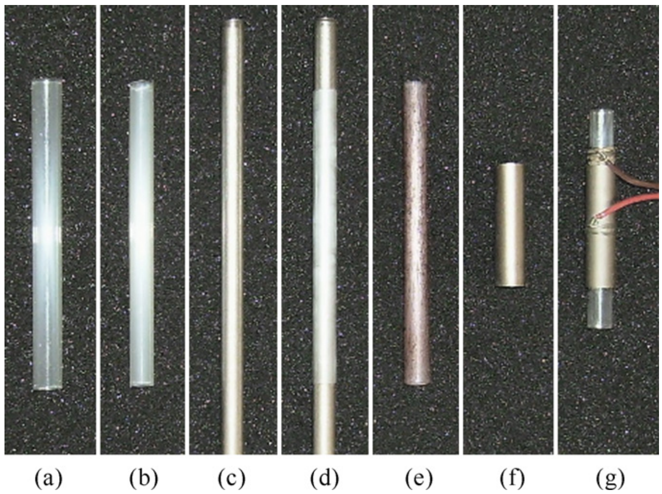

Fig. 3. Schematic showing the fabrication of the printhead chamber: (a) PET tube before shrink. (b) Teflon tube before etching. (c) The steel tube used as a mould during heating of PET. (d) PET tube after shrink. (e) Teflon tube after etching. (f) piezoelectric tube. (g) Shrunken PET tube bonded to the piezoelectric tube.

(CW2400, from ITW Chemtronics Inc.), forming the printhead chamber.

In the next step, two wires are separately attached to the inner and outer wall of the piezoceramic tube by using electrical conductive epoxy, for connecting the printhead to the piezo driver, as shown in Fig. 3g. Then the whole part is fixed inside a brass housing by araldite epoxy adhesive for protection. The solidified araldite epoxy can also prevent short circuit which can be caused by liquid permeation to the piezoceramic tube. The two connecting wires are pulled out through a hole in the housing, and the hole is also sealed with araldite epoxy, as shown in Fig. 2b. An outside thread is cut on the bottom of the brass housing for connecting the housing to the nozzle adaptor. Fig. 4 schematically shows the design of the brass housing and the nozzle adaptor.

2.2. Interchangeable nozzle design

The nozzle is fabricated by heating and pulling a glass tube, as demonstrated by Lee [17]. The setup is graphically shown in Fig. 5a.

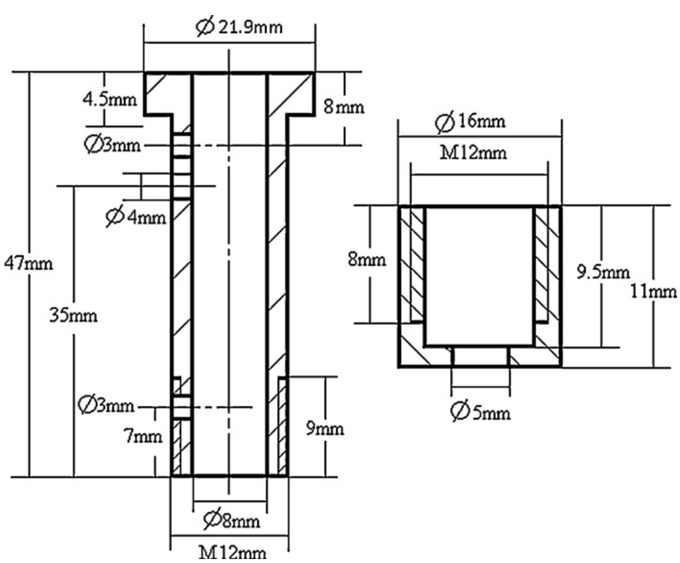

Fig. 4. Schematic showing the design of the printhead housing and the nozzle adaptor.

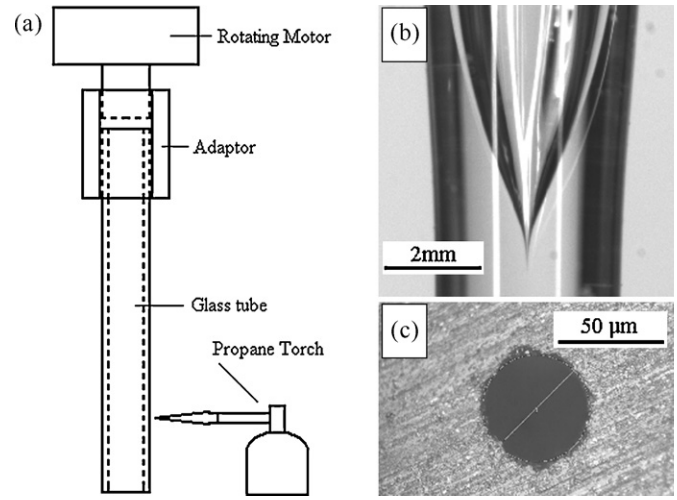

Fig. 5. Fabrication of a glass nozzle by pulling glass tubing. (a) Drawing of the glass tubing heating system (out of proportion). (b) Glass tubing containing a hollow cone with a closed end. (c) A 50 μm orifice fabricated by polishing the end of the tubing showing in (b).

A glass tube with 5.0 mm OD and 3.5 mm ID is vertically fixed to a motor which rotates the tube about its axis. By applying local heat to the lower section of the rotating glass with a propane torch, the glass tube is melted at the location of the flame, and pulled longer by the weight of its lower portion until it finally breaks into two parts, each of which contains a hollow cone with a closed end. The closed end is then polished by fine sand papers until an orifice of a desired diameter is exposed, as shown in Fig. 5c. By this method, orifices of 13–300 μm have been fabricated in this study. A similar glass-fabricated nozzle was also adopted by Fan et al. [18].

As recommended by Lee [17], to generate an axisymmetric conical nozzle profile, the rotation speed of the motor is maintained around 600 rpm.

The major advantage of this nozzle fabrication method is ease of manufacture and low cost. However, it is difficult to precisely control the taper angle of the nozzle and the size of the orifice. Nozzles with more controllable profile and accurate size can be fabricated by electrical discharge machining (EDM), silicon micromachined technology [19,20] and laser drilling.

Fig. 2 also shows how the interchangeable nozzle design is implemented. After being fixed to a short brass cylinder (cap 2 in Fig. 2) by araldite epoxy adhesive, the nozzle is placed inside another brass cap (cap 1 in Fig. 2) that has an inside thread which is tightly fitted to the outside thread of the printhead chamber. An O-ring must be used here to prevent cracking of the nozzle from overtightening of the threads.

3. Experimental testing of the new printhead

3.1. Experimental setup

Experimental tests were carried out to investigate the characteristics and repeatability of the PET/PTFE-based printhead, as well as to compare the ejection capacity of the PET/PTFE-based and the glass-based printheads.

The experimental setup is comprised of an air compressor, a pressure regulator, a liquid reservoir, a piezoelectric actuated printhead, a piezo driver, a stroboscope light and a CCD camera, as shown in Fig. 6.

The fluid to be dispensed is filled into a 60 ml stainless steel reservoir which is mounted on a XYZ motion stage. The combination of the air compressor and the pressure regulator (AD 3000D,

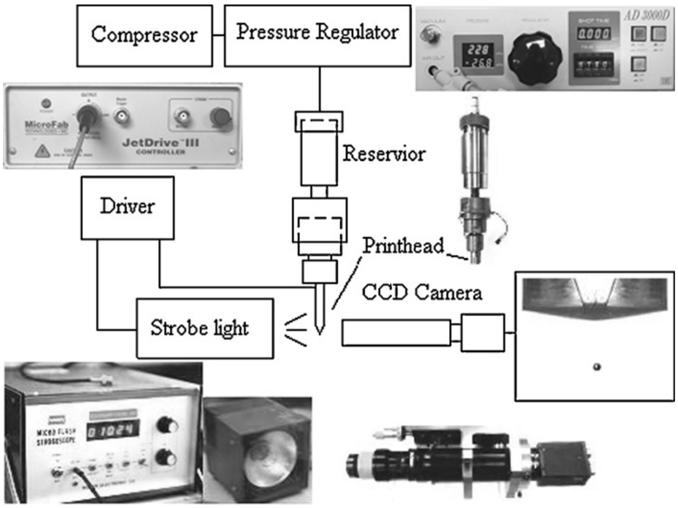

Fig. 6. Schematic showing of the drop-on-demand inkjet printing system used in the experiment.

from Iwashita Instruments Pte Ltd.) provides a negative pressure in the reservoir to hold up and prevent the liquid from leaking out of the orifice of the printhead. Before getting into the printhead, the liquid is filtered by passing it through a syringe filter with 0.2 μm pore size membrane (Ref. 4652, from Pall Corporation) to remove large particles which might block the nozzle. Electric signals are sent by a JetDrive^{TM}III (from Microfab Technologies Inc.) to the piezoelectric transducer, causing alternating expansion and contraction of the transducer as well as the printhead chamber, ultimately, squeezing the liquid inside the chamber and ejecting a droplet from the orifice.

The inkjet process is produced by a periodic driving voltage and the resulting droplet ejection is repeatable from one droplet to the next. This allows for stroboscopic imaging to determine the formation and the ejection velocity of the droplets. Signals are also sent by the driver to a stroboscope (MS-200, from Nissin Electronic Co., Ltd.) which has a pulse duration of 2 μs and is therefore capable of freezing an image of the high-speed droplet with minimum blur. The droplet shape is illuminated by the flashing of the strobe light and the images are captured by a JAI CV-A11 camera (from Ultravision Pte Ltd.). To determine the drop velocity, the stroboscope was operated at the same frequency as the printhead driver. By varying the time delay between the signal for the stroboscope and signal for the piezoelectric transducer, sequential images of the droplet during its motion are captured with known time differences. The drop velocity can then be derived by dividing the spacing between the droplets by the time difference between two frames. Fig. 7 shows a representative typical droplet formation sequence, the droplet is 50 μm and its velocity is 0.69 m/s.

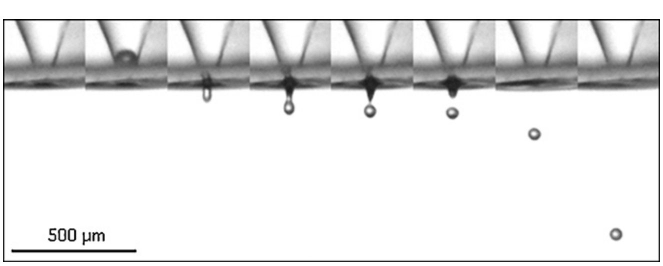

Fig. 7. Image sequences showing the formation of a 50 μm droplet from a 36 μm inkjet nozzle. The times shown are 0, 144, 322, 367, 389, 400, 522 and 1122 μs relative to the first frame. The drop velocity is here determined to be 0.69 m/s.

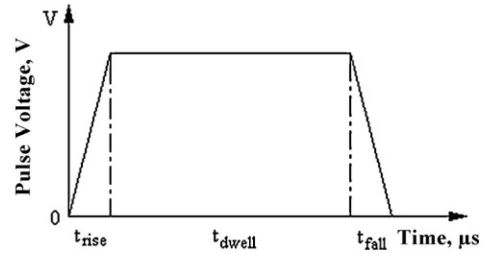

Fig. 8. Schematic showing of the uni-polar pulse waveform.

The droplet size is determined by two different methods, i.e. either measured directly from the images, or by a weight method. In the latter method, 7200 droplets are collected and then weighed for each test condition. Droplet diameter can then be calculated from its weight and the corresponding liquid density.

3.2. Experimental conditions

The jet driver made by Microfab Technologies Inc. is able to send out voltage pulses with designed profiles. Up to 12 points can be set to form the signal waveform. Commonly used signals are of uni-polar, bi-polar or sinusoidal shape. The maximum allowable amplitude and frequency for the pulse is ±140 V and 30 kHz, respectively.

Fig. 8 shows a uni-polar pulse employed in our experimental study. The zero line represents the equilibrium state of the piezoceramic tubing, without any external voltage. During the time of t_{rise}, the piezoceramic tubing expands outward to its maximum inner volume and holds that state for a time of t_{dwell}. During the time of t_{fall}, the piezoceramic tubing contracts inward, to its equilibrium state. The expansion and contraction of the piezoceramic tubing causes negative and positive pressure waves propagating and reflecting inside the printhead, which ultimately leads to droplet ejection [21]. During all the experiments, t_{rise} and t_{fall} were kept at 3 μs, which are the minimum permitted values of the jet driver, with the purpose of introducing instant action of the piezoeceramic tubing.

Static pressure needs to be applied to the reservoir, so that the liquid will not flow out of the nozzle under the hydrostatic pressure. The negative pressure applied to the reservoir was determined by direct observation showing no liquid leaking and no air entertainment.

3.3. Testing liquids

The conventional pigmented ink or standard dye-based ink for graphic printing normally has a viscosity of less than 5 cps. However, to apply inkjet printing in the new areas mentioned earlier in the introduction, various complex liquids like polymers, gels and other materials with much higher viscosities need to be effectively dispensed. Thus, aqueous glycerin solutions with viscosities from 1 cps to 120 cps are used to test our printhead.

4. Experimental results

4.1. Comparison of PET/PTFE-based and glass-based printhead

The commercial printheads fabricated by Dimatix, XAAR, Microfab and Microdrop can only dispense liquids with viscosity less than 20 cps [12]. In our printhead design, PET or Teflon tubing was used as the printhead chamber, but a separate glass-based printhead of similar configuration was also fabricated for this study to compare the dispensing capacity of the new type printhead and that of the glass-based printhead. Aqueous glycerin solutions with vis-

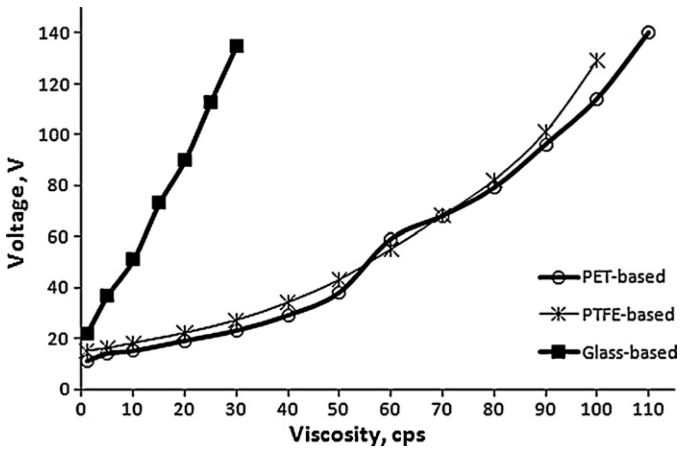

Fig. 9. Threshold voltages for PET-based printhead (○), PTFE-based printhead (*) and glass-based printhead (■). Nozzle diameter is 119 μm.

cosities from 1 cps to 120 cps were used for the test. Fig. 9 shows the threshold voltage needed for dispensing glycerin solutions of different viscosities. The same nozzle of 119 μm diameter was used for both of the PET/PTFE-based and glass-based printheads.

It can be seen that the threshold voltage increases with the increase of fluid viscosity, for all of the printheads. However, for the same viscosity, the PET/PTFE-based printhead requires a much smaller threshold voltage than the glass-based printhead. Furthermore, the PET/PTFE-based printhead can dispense liquids with viscosity of up to 100 cps, which far exceeds the performance of the glass-based ones which are typically used in commercial printheads.

The main reason for the lower voltage is that PET or Teflon is much softer than glass. When an electrical pulse is applied, the liquid chamber made of PET or Teflon tube is much easier to be squeezed by the piezoceramic element, thus less energy will be dissipated in the deformation of the liquid chamber. Consequently, a larger volumetric change will be realized in the liquid, leading to a better dispensing capacity.

Furthermore, from Eq. (1), for the piezoelectric tubes of the same wall thickness, the one with the larger diameter can generate a greater change in its volume. This is the reason why the self-fabricating glass-based printhead can only dispense glycerin solution with viscosity of 30 cps, which still exceeds the limitation of most commercial printheads. However, when the diameter of the piezoelectric tube increases, the diameter of the inner glass tube or PET/PTFE tube should also increase. Glass material is quite stiff and brittle; therefore, with the increase of its diameter, it becomes more fragile when the same wall thickness is used. However, with a thicker wall, more energy is absorbed in the glass and less volume change can be obtained. Fortunately, PET or Teflon is quite pliable; by adopting them as the printhead chamber, the piezoelectric tube with a bigger diameter can be used to further improve the printhead behavior for dispensing materials with high viscosity.

4.2. Effect of pulse width

For PET-based printhead, the effects of pulse width on droplet diameter and droplet velocity were investigated by keeping the pulse amplitude constant at 50 V. Note that here the pulse width represents the duration of t_{dwell} in Fig. 8. The jetting frequency was kept constant at 120 Hz. The PET-based printhead and PTFE-based printhead behave almost the same, for simplification, only the results for PET-based printhead will be discussed.

It is observed from Fig. 10 that both droplet velocity and droplet diameter initially increase with the increase of pulse width. The maximum droplet velocity 4.3 m/s is obtained when the pulse width reaches a value of 100 μs. Then droplet velocity rapidly decreases with a further increase of pulse width, reaching a minimum value of 1.2 m/s at 360 μs pulse width. The increase of droplet diameter continues until the pulse width is 120 μs. Then the droplet diameter is almost constant at a value of 188 μm until the pulse width reaches 270 μs, followed by a dramatic fall to the value of 135 μm. Both the droplet velocity and droplet diameter reach a near constant value after the pulse width exceeds 420 μs. With further increase of pulse width to 990 μs, air gets easily sucked into the nozzle, leading to a slight decrease of droplet velocity and droplet diameter. The reason for this air suction is that the piezoelectric element expands for a longer time when a waveform of a very large pulse width is applied. As a result, meniscus is pulled too far into the nozzle during each dispensing process, allowing air to be easily sucked into the nozzle, forming a void inside the nozzle. Furthermore, the nozzle used in the study does not have any hydrophobic treatment on the nozzle plate, thus a thin layer of ink will form on the nozzle plate during printing. The jet of droplets will cause a flow of ink towards the jet nozzle [22]. This pulled back ink from the ink layer on the nozzle plate closes the void, forming an air bubble inside the nozzle. Finally, a much bigger air bubble is formed inside the nozzle and totally stops the dispensing at a pulse width of 1160 μs. Single droplets without satellites can now be obtained in two ranges of pulse widths: 25–32 μs and 420–1130 μs.

4.3. Effects of voltage pulse amplitude

The effects of the pulse amplitude on the behavior of the PET-based printhead were investigated by dispensing 5 cps aqueous glycerin solution through a 119 μm nozzle. From Fig. 10, it can be seen that the optimal t_{dwell} for generating a high velocity droplet is 100 μs. Herein the t_{dwell} was kept constant at 100 μs. The pulse amplitude was varied to the maximum which can be generated by the jet driver, i.e. 140 V. The jetting frequency was kept constant at 120 Hz.

As shown in Fig. 11, both drop velocity and drop volume increase initially with an increase of pulse amplitude. However, single droplets can only be obtained using pulse amplitudes from 21 V to 40 V. Further increase in pulse amplitude generates a primary droplet followed by a small satellite droplet. This is understandable as a higher voltage causes a bigger volume change within the piezoelectric element, thus a longer column of liquid squeezed out and a satellite will be generated. The satellite droplet becomes bigger and tends to break into multiple satellite droplets as the pulse amplitude is further increased. The maximum droplet velocity is 3.24 m/s and the droplet diameter varies from 150 μm to 200 μm.

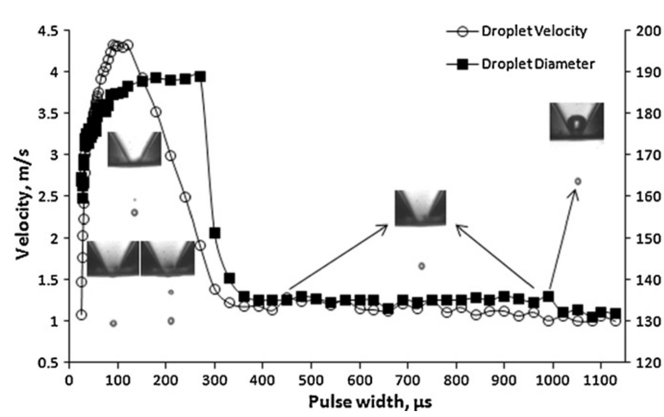

Fig. 10. Effects of pulse width on droplet velocity and droplet size. The pulse amplitude is 50 V. Nozzle diameter is 119 μm.

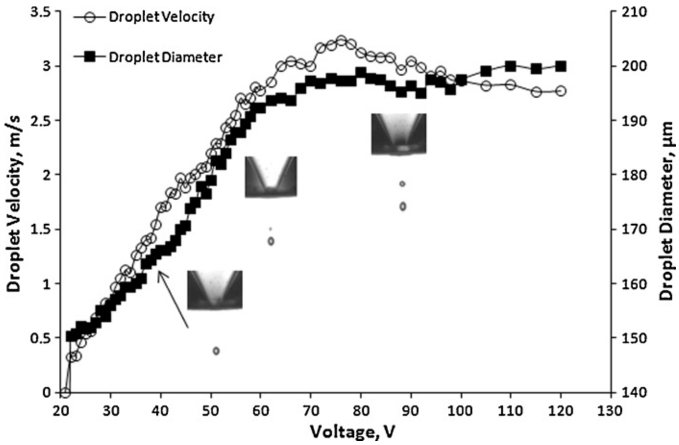

Fig. 11. Effects of pulse amplitude on droplet velocity and droplet size. The pulse width is 100 μs. Nozzle diameter is 119 μm.

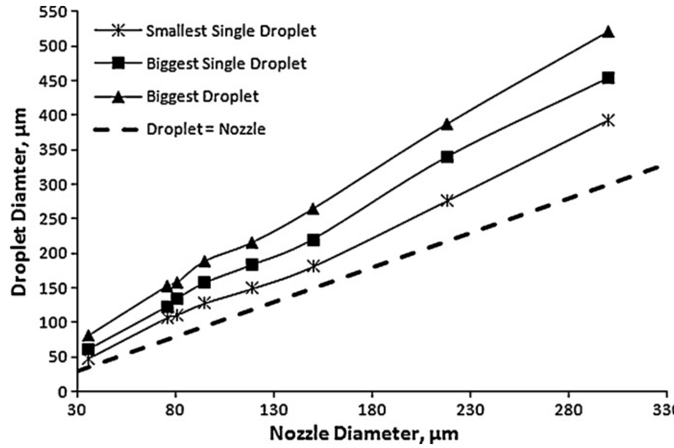

Fig. 12. Effects of nozzle size on droplet diameter. (*) the diameters of the smallest single droplets can be generated; (■) the diameters of the biggest single droplets can be generated; (▲) the diameters of the biggest droplets which can be generated using the maximum voltage.

A slight decrease in droplet velocity is observed once pulse amplitude exceeds 76 V. The reason for this decrease lies in the fact that: during the time t_{rise} and t_{dwell}, the piezoelectric element has expanded outward, resulting in a negative pressure in the printhead which causes the meniscus to move into the nozzle. When very high voltage is applied, the piezoelectric element expands more. As a result, meniscus is pulled too far into the nozzle during each dispensing process, allowing air to be easily sucked into the nozzle. The sucked air forms small air bubbles inside the nozzle which leads to the decrease of droplet velocity [23].

4.4. Nozzle size

For a specific printhead with a fixed nozzle size, it is of interest to determine the smallest droplet and the biggest droplet that can be generated.

Eight different nozzle sizes were investigated for this printhead. For each nozzle size, the pulse width was 22 μs. Then the pulse amplitude was slowly increased from 10 V to 140 V in steps of 1.0 V, until the liquid can be regularly dispensed. The corresponding droplet diameter is recorded as indicating for the smallest single droplet. The pulse amplitude was further increased, until satellite droplet was generated along with the main droplet. Then the pulse amplitude was decreased by 1 V step length and droplets were collected. Droplet diameter was calculated and recorded as that for the biggest regular droplets, i.e. without a satellite.

To determine the largest droplet, irrespective whether a satellite was produced, a different approach was used. In accordance with the results of Figs. 10 and 11, to obtain the biggest droplet diameter, the pulse amplitude was set to be 140 V. The pulse width was increased from 25 μs to 625 μs at intervals of 50 μs. Droplets were collected and weighed to determine their size. The biggest value among the 13 samples was recorded as the biggest droplet diameter.

Fig. 12 shows the relationship between the droplet size and the nozzle size, for all nozzles tested. It is shown that all the above three types of droplet sizes increase monotonically with increasing nozzle sizes. The droplets are always larger than the nozzle diameter indicated by the broken line. An excellent rule-of-thumb states that the droplets are between 120% and 220% of the nozzle diameter.

4.5. Repeatability

A good inkjet printhead should have nice repeatability, allowing generation of a rapid sequence of droplets without big variation in droplet velocity and droplet size. To test the repeatability of our novel PET-based printhead, water was dispensed through a 119 μm nozzle. In accordance with Fig. 10, to generate stable single droplets, the printing was carried out by using a signal of 50 V pulse amplitude and 600 μs pulse width. As shown in Fig. 13 over a one hour test run at 120 Hz, the variation in droplet diameter is only 0.18% and 0.46% for droplet velocity.

4.6. Maximum jetting frequency

As a manufacturing tool, high-speed jetting is required to increase productivity of inkjet printing technology. For industrial printer with multi-nozzle, this can be realized by increasing number of nozzles or increasing jetting frequency of each nozzle. While for printhead with single nozzle, as designed in this study (also for Microfab and Microdrop), jetting speed can only be improved by increasing jetting frequency. However, for a reliable jetting, the subsequent droplet should not be ejected until the pressure wave from the previous pulse signal has damped sufficiently. This damping takes time and thus limits the maximum jetting frequency [24]. For a specific printhead, its maximum jetting frequency is mainly depended on the construction of the printhead as well as the driving signal [25]. Typical DOD printheads generate droplets at rates in the range 0.1–10 kHz.

If a droplet is ejected before the pressure waves from the previous pulse signal have sufficiently damped, the new droplet ejection cycle will be affected by the non-zero flow field inside the printhead. Consequently, the droplet velocity and the droplet size will

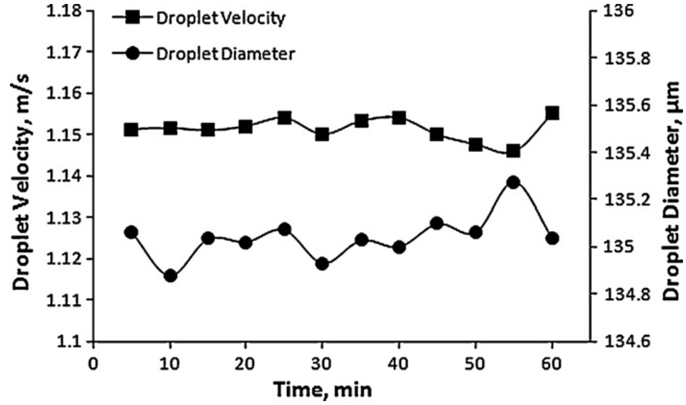

Fig. 13. Repeatability test of the PET-based printhead. Nozzle diameter is 119 μm.

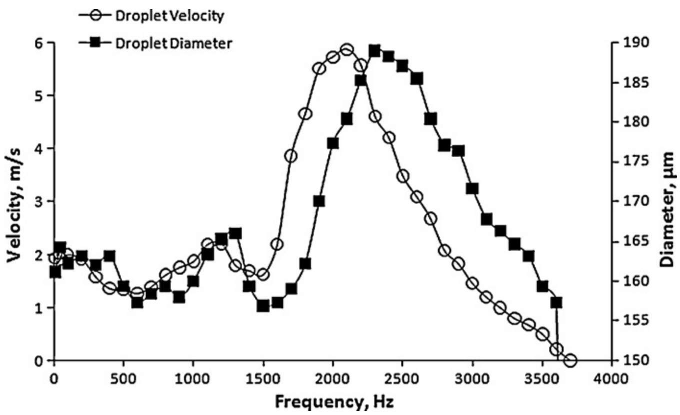

Fig. 14. Effects of jetting frequency on droplet velocity and droplet size. The pulse width is 100 μs. The pulse amplitude is 30 V. Nozzle diameter is 119 μm.

increase or decrease, depending on whether the residual movement of the meniscus is in-phase or out-of-phase with the new droplet ejection cycle [26].

Fig. 14 shows the effects of jetting frequency on droplet velocity and droplet diameter, for the PET-based printhead. Printing was carried out by dispensing water through a 119 μm nozzle. The t_{dwell} was kept constant at 100 μs, the optimal value for the printhead. The pulse amplitude was kept constant at 30 V. The driving frequency was varied from 1 Hz to 5 kHz. It is shown that below 1.5 kHz, jetting frequency has relatively small effects on drop velocity and drop diameter. The reason was that below this frequency, there was sufficient time (670 μs, according to a jetting frequency of 1.5 kHz) between droplet ejection cycles for the acoustic pressure waves to get damped. Thus the droplet ejection cycles were independent of each other and were irrelevant with the jetting frequency.

However, when jetting frequency exceeds 1.5 kHz, both drop velocity and drop volume rapidly increase with an increase of jetting frequency. The maximum droplet velocity 5.7 m/s is obtained when the jetting frequency reaches a value of 2.1 kHz. Then droplet velocity decreases with a further increase of jetting frequency. The increase of droplet diameter continues until the jetting frequency is 2.3 kHz. Then the droplet diameter also decreases with a further increase of jetting frequency. The dispensing fails at a frequency of 3.7 kHz. This maximum jetting frequency of 3.6 kHz is higher than that of the Microdrop printhead (2.0 kHz), while much lower than that of the Dimatix, XAAR, and Microfab printhead (20 kHz).

The strong variation of droplet velocity and droplet diameter with changing of jetting frequency indicates that, above 1.5 kHz, the time interval between two consecutive droplet ejection cycles was not sufficiently long for the acoustic pressure waves to get adequately damped. With the meniscus motion method proposed by Kwon [27], one can estimate the time needed for the damping of the pressure waves. For the printhead designed in our study, it has an optimal t_{dwell} around 100 μs; and it takes around 800–1000 μs for the acoustic pressure waves to get sufficiently damped. As a result, our printhead should has a much lower threshold frequency [26], above which jetting frequency will have great effects on droplet speed as well as droplet volume. This is verified by the experiment results, as shown in Fig. 14. The threshold frequency for the designed printhead is only 1.5 kHz.

The maximum droplet velocity is produced with a driving frequency of around 2.1 kHz, corresponding to the resonance frequency of the inkjet channel. This resonance frequency is much lower as compared to other commercial printheads. The reason is that the first mode resonance frequency of the printhead is inversely proportional to the length of the pressure channel [26]; in the meantime, the designed printhead has a liquid channel of 50 mm length, which is much larger than that of the commercial printheads. As a result, a much lower resonance frequency is reasonably expected.

5. Conclusions

A PET/PTFE-based piezoelectric DOD inkjet printhead with an interchangeable nozzle design has been proposed and fabricated by the authors. The printhead chamber is made of PET or Teflon tube, which is much softer than the commonly used glass tube. The ejecting capacity of this novel printhead has been compared with commercial printheads, and found to have superior performance and versatility. Aqueous glycerin solutions with viscosity as high as 100 cps have been successfully dispensed, while the corresponding commercial printheads can only dispense liquids with viscosities lower than 20 cps. PTFE-based printhead provides excellent anti-corrosive property when strongly corrosive inks are involved. The interchangeable nozzle design largely alleviates the difficulty in cleaning of clogged nozzles and greatly reduces the occurrence of printhead damage. The effects of operating parameters, including voltage pulse amplitude, pulse width and jetting frequency, on droplet size and droplet velocity have been characterized. The new printhead shows excellent repeatability.

Acknowledgements

The authors would like to thank Mr. Zhou Jinxin and Mr. Thian Chen Hai, Stanley for their continuous support and helpful discussion. Funding was provided by A-STAR grant R-265-000-224-305.

References

[1] Z.C. Liu, Y. Su, K. Varahramyan, Inkjet-printed silver conductors using silver nitrate ink and their electrical contacts with conducting polymers, Thin Solid Films 478 (2005) 275–279.
[2] H. Sirringhaus, T. Kawase, R.H. Friend, T. Shimoda, M. Inbasekaran, W. Wu, E.P. Woo, High-resolution inkjet printing of all-polymer transistor circuits, Science 290 (2000) 2123–2126.
[3] R.A. Street, W.S. Wong, S.E. Ready, M.L. Chabinyc, A.C. Arias, S. Limb, A. Salleo, R. Lujan, Jet printing flexible displays, Mater. Today 9 (2006) 32–37.
[4] W. Feng, J.Y.H. Fuh, Y.S. Wong, Development of a drop-on-demand micro dispensing system, Mater. Sci. Forum (Switzerland) (2006).
[5] P. Calvert, Printing cells, Science 318 (2007) 208–209.
[6] R.E. Saunders, J.E. Gough, B. Derby, Delivery of human fibroblast cells by piezoelectric drop-on-demand inkjet printing, Biomaterials 29 (2008) 193–203.
[7] M. Nakamura, A. Kobayashi, F. Takagi, A. Watanabe, Y. Hiruma, K. Ohuchi, Y. Iwasaki, M. Horie, I. Morita, S. Takatani, Biocompatible inkjet printing for designed seeding of individual living cells, Tissue Eng. 11 (2005) 1658–1666.
[8] B.M. Wu, S.W. Borland, R.A. Giordano, L.G. Cima, E.M. Sachs, M.J. Cima, Solid free-form fabrication of drug delivery devices, J. Control. Release 40 (1996) 77–87.
[9] T. Kawase, T. Shimoda, C. Newsome, H. Sirringhaus, R.H. Friend, Inkjet printing of polymer thin film transistors, Thin Solid Films 438–439 (2003) 279–287.
[10] K.X. Steirer, J.J. Berry, M.O. Reese, M.F.A.M. van Hest, A. Miedaner, M.W. Liberatore, R.T. Collins, D.S. Ginley, Ultrasonically sprayed and inkjet printed thin film electrodes for organic solar cells, Thin Solid Films 517 (2009) 2781–2786.
[11] D. Xu, V. Sanchez-Romaguera, S. Barbosa, W. Travis, J. de Wit, P. Swan, S.G. Yeates, Inkjet printing of polymer solutions and the role of chain entanglement, J. Mater. Chem. 17 (2007) 4902–4907.
[12] B.J. de Gans, P.C. Duineveld, U.S. Schubert, Inkjet printing of polymers: state of the art and future developments, Adv. Mater. 16 (2004) 203–213.
[13] A.U. Chen, O.A. Basaran, A new method for significantly reducing drop radius without reducing nozzle radius in drop-on-demand drop production, Phys. Fluids 14 (2002) L1–L4.
[14] A.A. Goghari, S. Chandra, Producing droplets smaller than the nozzle diameter by using a pneumatic drop-on-demand droplet generator, Exp. Fluids 44 (2008) 105–114.
[15] E.Q. Li, S.T. Thoroddsen, J.Y.H. Fuh, S.C.H. Thian, Y.S. Wong, H.T. Loh, L. Lu, PET-based piezoelectric squeeze mode microjetting printhead with interchangeable nozzles, Provisional US Patent 61/226781 (2009).
[16] S.L. Zoltan, Pulse droplet ejection system, US Patent 3683212 (1974).
[17] E.R. Lee, Microdrop Generation, CRC Press, New York, 2002.
[18] K.C. Fan, J.Y. Chen, C.H. Wang, W.C. Pan, Development of a drop-on-demand droplet generator for one-drop-fill technology, Sens. Actuators A 147 (2008) 649–655.

[19] G. Percin, B.T. Khuri-Yakub, Micromachined droplet ejector arrays for controlled ink-jet printing and deposition, Rev. Sci. Instrum. 73 (2002) 2193–2196.
[20] Y. Wang, J. Bokor, A. Lee, Maskless lithography using drop-on-demand inkjet printing method, Proc. SPIE 5374 (2004) 628–636.
[21] D.B. Bogy, F.E. Talke, Experimental and theoretical study of wave propagation phenomena in drop-on-demand inkjet devices, IBM J. Res. Dev. 28 (1984) 314–321.
[22] B. Beulen, J. de Jong, H. Reinten, M. van den Berg, H. Wijshoff, R. van Dongen, Flows on the nozzle plate of an inkjet printhead, Exp. Fluids 42 (2007) 217–224.
[23] J. de Jong, R. Jeurissen, H. Borel, M. van den Berg, H. Wijshoff, H. Reinten, M. Versluis, A. Prosperetti, D. Lohse, Entrapped air bubbles in piezo-driven inkjet printing: their effect on the droplet velocity, Phys. Fluids 18 (2006) 121511.
[24] M.A. Groninger, P.G.M. Kruijt, H. Reinten, R.H. Schippers, J.M.M. Simons, Method of controlling an inkjet printhead, an inkjet printhead suitable for use of said method, and an inkjet printer comprising said printhead, US Patent 7,357,474 (2008).
[25] K.S. Kwon, W. Kim, A waveform design method for high-speed inkjet printing based on self-sensing measurement, Sens. Actuators A 140 (2007) 75–83.
[26] H. Wijshoff, Structure- and fluid-dynamics in piezo inkjet printheads, Ph.D. Thesis, University of Twente, The Netherlands, 2008.
[27] K.S. Kwon, Methods for detecting air bubble in piezo inkjet dispensers, Sens. Actuators A 153 (2009) 50–56.

Biographies

Er-Qiang Li received the BS degree in energy and power engineering from Xi'an Jiaotong University in 2005. Currently he is working toward the PhD degree at National University of Singapore. His research interests include microdrop generation technology and cell printing.

Qian Xu received her MS degree in mechanical engineering from National University of Singapore in 2008, MS degree in mechanical engineering from Sichuan University in 2008, and BS degree in manufacturing from Sichuan University in 2005. Her research interest is microdrop generation technology.

Jie Sun received her B. Eng. degree and M. Eng. degree from Dalian University of Technology, China, and PhD degree from National University of Singapore. Currently, she is a lecturer with National University of Singapore. Her research interests include bio-coating fabrication, condition monitoring, and mechatronic system.

Y.H. Fuh received his PhD degree in mechanical engineering from the University of California at Los Angeles (UCLA) in 1992, MS degree in manufacturing engineering from UCLA in 1985, and BS degree in mechanical engineering from the National Chiao Tung University, Taiwan in 1980. He is currently a full professor at the Department of Mechanical Engineering, National University of Singapore (NUS). His research interests include collaborative engineering, digital manufacturing and micro/bio-fabrication. He is a fellow of ASME and SME, a certified manufacturing engineer (CMfgE) from CASA/SME and a registered professional engineer (PE) in manufacturing engineering from California, USA. He serves as an associate editor, guest editor and editorial board member in many manufacturing related journals. He has published more than 160 journal papers, 150 conference papers, authored 2 monographs, and owns 6 patents and delivered many invited talks in conferences and institutions.

Y.S. Wong is professor in the mechanical engineering Department of the National University of Singapore (NUS). His research interests are in manufacturing process characterization for modeling, monitoring, control and optimization, and product data capture and processing for design and manufacture. In these areas, he has published in refereed journals and proceedings of international conferences, contributed to books, and participated in several local and overseas collaborative projects.

S.T. Thoroddsen received his BS degree from University of Iceland and an MS degree from Colorado State University, before completing his PhD in applied mechanics from University of California, San Diego. He subsequently held professorships at University of Illinois at Urbana-Champaign and National University of Singapore, before joining King Abdullah University of Science and Technology in 2009. His research focuses on high-speed imaging in fluid mechanics, such as drop and bubble dynamics.